Mislocalization of DNAH5 and DNAH9 in Respiratory Cells from Patients with Primary Ciliary Dyskinesia

Manfred Fliegauf, Heike Olbrich, Judit Horvath, Johannes H. Wildhaber, Maimoona A. Zariwala, Marcus Kennedy, Michael R. Knowles, and Heymut Omran

Department of Pediatrics and Adolescent Medicine, University Hospital Freiburg, Freiburg, Germany; Swiss Pediatric Respiratory Physiology Research Group, Department of Respiratory Medicine, University Children's Hospital, Zürich, Switzerland; and Department of Medicine, University of North Carolina, Chapel Hill, North Carolina

Rationale: Primary ciliary dyskinesia (PCD) is a genetically heterogeneous disorder characterized by recurrent infections of the airways and situs inversus in half of the affected offspring. The most frequent genetic defects comprise recessive mutations of *DNAH5* and *DNAI1*, which encode outer dynein arm (ODA) components. Diagnosis of PCD usually relies on electron microscopy, which is technically demanding and sometimes difficult to interpret. *Methods:* Using specific antibodies, we determined the subcellular localization of the ODA heavy chains DNAH5 and DNAH9 in human respiratory epithelial and sperm cells of patients with PCD and control subjects by high-resolution immunofluorescence imaging. We also assessed cilia and sperm tail function by high-speed video microscopy. *Results:* In normal ciliated airway epithelium, DNAH5 and DNAH9 show a specific regional distribution along the ciliary axoneme, indicating the existence of at least two distinct ODA types. DNAH5 was completely or only distally absent from the respiratory ciliary axoneme in patients with PCD with *DNAH5*− (n = 3) or *DNAI1*− (n = 1) mutations, respectively, and instead accumulated at the microtubule-organizing centers. In contrast to respiratory cilia, sperm tails from a patient with *DNAH5* mutations had normal ODA heavy chain distribution, suggesting different modes of ODA generation in these cell types. Blinded investigation of a large cohort of patients with PCD and control subjects identified DNAH5 mislocalization in all patients diagnosed with ODA defects by electron microscopy (n = 16). Cilia with complete axonemal DNAH5 deficiency were immotile, whereas cilia with distal DNAH5 deficiency showed residual motility. *Conclusions:* Immunofluorescence staining can detect ODA defects, which will possibly aid PCD diagnosis.

Keywords: fluorescent antibody technique; genetics; respiratory tract diseases

Primary ciliary dyskinesia (PCD; OMIM 242650) represents a rare autosomal recessive disorder affecting 1 in 20,000 individuals (1). Clinical manifestations include recurrent infections of the upper and lower respiratory tract, caused by reduced mucociliary clearance; sperm immobility; and situs inversus in half of the affected offspring, caused by randomization of left–right asymmetry (2). Chronic airway disease often leads to bronchiectasis and can progress to respiratory failure. The PCD phenotype results from axonemal abnormalities and dysfunction of motile cilia and flagella. Cilia and flagella are hairlike organelles extending from the cell surface. In vertebrates, multiple motile cilia or motile monocilia are located on various epithelial cells and move extracellular fluid (3). These include the respiratory epithelium of the airways (respiratory cilia), the embryonic node (primary cilia), and the ependyma of the brain ventricles (ependymal cilia). The sperm tail (flagellum) propels the sperm cell through liquid. The involvement of motile cilia in diverse processes such as left–right axis pattern formation, cerebrospinal fluid flow, and mucociliary clearance shows that they have been adapted as versatile tools for many biological processes (1–3).

Respiratory cilia and sperm flagella consist of a highly ordered basic structure of nine peripheral microtubule doublets composed of an A-tubule and a B-tubule arranged around two central microtubules (9+2 axoneme). Axonemal dyneins are the molecular motors that generate microtubule sliding and thus the movement of motile cilia and flagella by ATPase-dependent reactions (1). Dynein heavy chain proteins assemble with intermediate and light chains into large multiprotein complexes to form inner and outer dynein arms (ODAs), respectively, which are attached to the peripheral axonemal A-microtubules (4–6). The dynein heavy chains form the globular heads and the stem of the complexes and contain the ATPase and microtubule motor domains.

We have previously localized a PCD locus to chromosome 5p, which contains *DNAH5*, the human ortholog of the *Chlamydomonas* ODA γ-heavy chain gene (7, 8). Recessive mutations of *DNAH5* result in nonfunctional DNAH5 proteins (9). Affected patients have dysmotile respiratory cilia with ODA defects. Mutations in *DNAI1*, encoding an ODA intermediate chain orthologous to *Chlamydomonas* IC78, also cause ODA defects in patients with PCD (10, 11).

To gain insight into the molecular mechanisms by which *DNAH5*− and *DNAI1*− mutations lead to dysfunction of motile cilia we analyzed human ciliated respiratory epithelial cells by immunofluorescence imaging, using antibodies against specific ODA components. We demonstrate that human respiratory cilia contain at least two different ODA types. Our data provide the first evidence that mislocalization of ODA proteins within the respiratory cells is a frequent finding in patients with PCD with ODA deficiency. It is possible that this immunofluorescence-based method could aid PCD diagnosis. In addition, the observation of DNAH5 absence within the respiratory ciliary compartment but normal DNAH5 distribution within the sperm flagellum of a patient with *DNAH5* mutations raises the possibility that both organelle types are assembled by distinct mechanisms.

METHODS

Patients and Families

Signed and consent forms were obtained from patients and family members, using protocols approved by the Institutional Ethics Review Board of the University of Freiburg (Freiburg, Germany) and collaborating institutions. We obtained transnasal brush biopsies from a large

cohort of patients fulfilling diagnostic criteria of PCD. Two patients with cystic fibrosis, 3 with recurrent respiratory infections, and 10 healthy volunteers were included as control subjects (Table 1). Samples were evaluated in a blinded fashion to avoid investigator bias.

Generation of DNAH5-specific Antibodies

Antibodies, raised in rabbits against amino acids 42–325 of DNAH5, were expressed as a glutathione *S*-transferase fusion protein (GE Healthcare/Amersham Biosciences, Freiburg, Germany) in *Escherichia coli*. Antibodies were affinity purified in a maltose-binding protein fusion system (New England BioLabs, Frankfurt, Germany).

Immunoblotting

Axonemal protein extracts were prepared from a pig trachea according to previously published procedures (12, 13). Proteins were separated on a NuPAGE 3–8% TRIS–acetate gel (Invitrogen, Karlsruhe, Germany) and blotted onto a polyvinylidene difluoride membrane (GE Healthcare/ Amersham Biosciences). The blot was processed for ECL Plus (GE Healthcare/Amersham Biosciences) detection, using DNAH5 antibody (diluted 1:1,000) and horseradish peroxidase-conjugated anti-rabbit antibody (diluted 1:2500; Santa Cruz Biotechnology, Heidelberg, Germany).

Immunofluorescence Analysis

Respiratory epithelial cells were obtained by transnasal brush biopsy (Cytobrush Plus; Medscand Medical, Malmö, Sweden) and suspended in cell culture medium. Sperm cells were washed with phosphate-buffered saline. Samples were spread onto glass slides, air dried, and stored at –80°C until use. Cells were treated with 4% paraformaldehyde, 0.2% Triton X-100, and 0.5% skim milk before incubation with primary antibody (at least 2 hours) and secondary antibody (30 minutes) at room temperature. Appropriate controls were performed by omitting the primary antibody. Commercially available primary antibodies were as follows: mouse anti–acetylated α-tubulin and mouse anti–γ-tubulin (Sigma, Taufkirchen, Germany), and mouse anti-DNAH9 (BD Biosciences, Heidelberg, Germany). Anti-DNAH9 antibodies have been previously described (12). We confirmed the specificity by Western blot, which demonstrated a specific dynein heavy chain band distinct from the DNAH5 band (data not shown). Secondary antibodies (Alexa Fluor 488 and Alexa Fluor 546) were from Molecular Probes/Invitrogen (Eugene, OR). DNA was stained with Hoechst 33342 (Sigma). Confocal images were taken with a Zeiss LSM 510 (Carl Zeiss, Oberkochen, Germany).

High-speed Video Analysis of Ciliary Beat Frequency

Ciliary beat frequency was assessed with the Sisson–Ammons video analysis (SAVA) system (Ammons Engineering, Mt. Morris, MI) (14). Transnasal brush biopsies were immediately viewed with an Olympus IMT-2 microscope (×40 phase-contrast objective) equipped with an ES-310 Turbo monochrome high-speed video camera (Redlake, San Diego, CA) set at 125 frames per second. The ciliary beat pattern was evaluated on slow-motion playbacks.

RESULTS

Evidence of Distinct ODA Types in Respiratory Cilia

To investigate molecular mechanisms responsible for dysfunction of motile human respiratory cilia we raised antibodies against DNAH5. Western blot of a mammalian axonemal extract specifically detected a single band of about 500 kD, which corresponds to the predicted molecular mass of DNAH5 (Figure 1A). We next analyzed the distribution of DNAH5 in human respiratory cilia *in vivo* by immunofluorescence staining of transnasal brush biopsies from healthy donors. As controls we used antibodies against the cilia-specific acetylated α-tubulin isoform. DNAH5 staining was observed throughout the respiratory ciliary axoneme (Figure 1), indicating that assembled ODAs along the entire length of the axoneme contain DNAH5. This is consistent with previous ultrastructural analyses showing ODAs being assembled only at the peripheral microtubule doublets (15, 16). In addition, we observed staining of DNAH5 in the distal

region of the basal body, where it colocalizes with γ-tubulin, a marker of the microtubule-organizing centers adjacent to the basal body foot (17). We regularly observed specific DNAH5 staining in the apical perinuclear region and in cytoplasmic compartments, which connect the perinuclear region with the microtubule-organizing centers (Figures 1B and 1C). We also investigated the spatial distribution of a second ODA heavy chain DNAH9, which is the ortholog of the *Chlamydomonas* ODA β-heavy chain (12). In respiratory epithelial cells DNAH9 antibodies exclusively stained the distal two-thirds of the cilia (Figure 2A). These findings demonstrate that in respiratory cilia at least two ODA types are present. Proximal ODA complexes are DNAH9 negative and DNAH5 positive (Type 1), whereas distal ODA complexes contain DNAH9 and DNAH5 (Type 2). Interestingly, in contrast to DNAH5, DNAH9 staining was almost undetectable in the cytoplasm and appeared diffuse, if distinguishable from background signals (Figure 2A). Moreover, we did not observe DNAH9 staining of the basal body and microtubule-organizing centers.

DNAH5 and *DNAI1* Mutations Can Cause Deficiency of ODA Components within the Ciliary Compartment

We have previously reported (9) that PCD patients with ODA defects of families F373 (1855NfsX5), F658 (2814fsX1), and UNC7 (splice acceptor site mutation predicting deletion of exon 75) carry homozygous *DNAH5* mutations (Table 1). To gain insight into the mechanism by which *DNAH5* mutations disrupt normal cilia function *in vivo*, we analyzed respiratory epithelial cells from these patients by immunofluorescence staining. DNAH5 proteins were undetectable in the ciliary axonemes of these patients with PCD (Figures 3A–3C). Instead, DNAH5 mutant proteins accumulated at the microtubule-organizing centers. Therefore, mutated DNAH5 is still expressed but unable to localize to the ciliary axoneme. We did not observe any DNAH9 staining of the ciliary compartment in the three patients with known *DNAH5* mutations (Figure 3E). Thus, the three studied *DNAH5* mutations affect at least two ODA complexes (Type 1 and Type 2), because DNAH5 and DNAH9 are absent within the ciliary compartment.

We next investigated whether mutations of the axonemal ODA intermediate chain gene *DNAI1*, which cause PCD with ODA defects (11, 18), result in similar localization defects of the ODA heavy chain components DNAH5 and DNAH9. Surprisingly, in respiratory epithelial cells from patient UNC119, who carries compound heterozygous *DNAI1* mutations (219+ 3insT/W568X) (19), DNAH5 staining was moderate in the proximal part but absent from the distal part of the ciliary compartment (Figure 3F). Furthermore, *DNAI1* mutations also caused DNAH5 to accumulate at the microtubule-organizing centers and within cytoplasmic compartments. DNAH9 was absent within the ciliary axonemes from patient UNC119 and weak within the cytoplasm (data not shown). In the studied patient DNAI1 mutant proteins do not inhibit transfer of DNAH5 molecules to the ciliary compartment per se. Absence of DNAH5 and DNAH9 in the distal ciliary compartment suggests that DNAI1 mutant proteins affect Type 2 ODA complexes in this patient.

We noted variable degrees of acetylated α-tubulin staining of the perinuclear region in both control and mutant respiratory cells (Figures 1C and 3A–3C). Therefore, the staining pattern was not influenced by *DNAH5* or *DNAI1* mutations.

DNAH5 Staining Can Detect ODA Defects

The characteristic DNAH5 staining pattern of *DNAH5* or *DNAI1* mutant respiratory cells prompted us to test whether immunofluorescence staining can generally detect ODA defects.

TABLE 1. CLINICAL, FUNCTIONAL, ULTRASTRUCTURAL, IMMUNOFLUORESCENCE, AND MUTATIONAL DATA OF PATIENTS WITH PCD AND CONTROL INDIVIDUALS

Identity	Origin	Clinical Status	Cilia Beat Frequency and Pattern	EM ODA Defect	Mutational Status	Immunofluorescence Staining*		
						DNAH5 in Cilia	DNAH5 in MTOC	DNAH9 in Cilia
F373II3	Lebanon	PCD, immotile sperm, oligozoospermia	Immotile	Yes	*DNAH5* homozygous 5563insA	—	+	—
F373II4	Lebanon	PCD, SI, azoospermia	Immotile	Yes	*DNAH5* homozygous 5563insA	—	+	—
F658	Germany	PCD, SI	Immotile	Yes	*DNAH5* homozygous 8440delGAACCAAA	—	+	—
UNC7	USA	PCD	< 1 Hz, limited range, uncoordinated	Yes	*DNAH5* hom IVS74-1G→C	—	+	—
UNC119	USA	PCD	< 1Hz, limited range, uncoordinated	Yes	*DNAI1* compound heterozygous 219+3insT/W568X	Proximal, +; distal, —	+	—
OP4 II	Germany	PCD	Immotile	Yes	ND	—	+	—
F649II2	Germany	PCD, SI	Immotile	Yes	ND	—	+	ND
F651	Germany	PCD, SI	1–3 Hz, limited range, uncoordinated	Yes	ND	Proximal, +; distal, —	+	ND
OP50	Switzerland	PCD	Immotile	Yes	ND	—	+	ND
OP51II1	Switzerland	PCD	Immotile	Yes	ND	—	+	ND
OP51II2	Switzerland	PCD, SI	Immotile	Yes	ND	—	+	ND
OP54	Switzerland	PCD, SI	Immotile	Yes	ND	—	+	ND
OP55	Switzerland	PCD	Immotile	Yes	ND	—	+	ND
UNC646	USA	PCD	< 1 Hz, limited range, uncoordinated	Yes	ND	—	+	ND
UNC16	USA	PCD	< 1 Hz, limited range, uncoordinated	Yes	*DNAH5* and *DNAI1* excluded	—	+	ND
UNC17	USA	PCD, SI	ND	Yes	*DNAH5* and *DNAI1* excluded	—	+	ND
OP40II	Germany	PCD, SI	Immotile	ND	ND	—	+	—
OP66	Germany	PCD, SI	max 1–2 Hz, limited range, uncoordinated	ND	ND	—	+	ND
OP74	Germany	PCD, SI	Immotile	ND	ND	—	+	ND
OP80II1	Germany	PCD	ND	ND	ND	—	+	ND
F718II	Germany	PCD	max 1–2 Hz, limited range, uncoordinated	ND	ND	Proximal, +; distal, —	+	ND
OP6	Germany	PCD, SI	max 3–4 Hz, limited range, uncoordinated	ND	ND	Proximal, +; distal, —	+	ND
OP25	Turkey	PCD, SI	max 3–5 Hz, limited range, uncoordinated	ND	ND	Proximal, +; distal, —	+	ND
OP46	Switzerland	PCD, SI	Immotile	ND	ND	Proximal, +; distal, —	+	ND
OP56II3	Germany	Healthy proband	max 9 Hz, coordinated	ND	ND	+	+	ND
OP23II1	Germany	Recurrent respiratory infections	max 7 Hz, coordinated	ND	ND	+	+	ND
OP52	Switzerland	Recurrent respiratory infections	max 9 Hz, coordinated	Normal	ND	+	+	ND
OP53	Switzerland	Recurrent respiratory infections	max 8 Hz, coordinated	ND	ND	+	+	ND
UNC129	USA	Cystic fibrosis	ND	ND	CFTR mutation	+	+	ND
UNC130	USA	Cystic fibrosis	ND	ND	CFTR mutation	+	+	ND
OP47	Switzerland	PCD	max 6 Hz, limited range, uncoordinated	Only IDA	ND	+	+	ND
UNC2	USA	PCD	10 Hz, limited range, uncoordinated	Only IDA	ND	+	+	ND

Definition of abbreviations: CFTR = cystic fibrosis transmembrane regulator; EM = electron microscopy; Hz = hertz; IDA = inner dynein arm; max = maximum; MTOC = microtubule organizing center; ND = not determined; ODA = outer dynein arm; PCD = primary ciliary dyskinesia; SI = situs inversus.
 Data from OP56II3 (healthy proband) is shown representatively for a total of 10 control individuals. Immotile cilia did not show any motion.
 * +, positive staining; —, absent staining.

For that purpose we investigated a large cohort comprising patients fulfilling diagnostic criteria of PCD and control individuals in a blinded fashion. All of the 16 patients with PCD previously diagnosed by electron microscopy for ODA defects as well as further 8 patients with unknown ultrastructural diagnosis showed complete or distal absence of DNAH5 staining in the ciliary axonemes and accumulation of DNAH5 at the microtubule-organizing centers (Table 1). In contrast, all 15 control individuals, including 2 patients with cystic fibrosis, 3 patients with recurrent respiratory infections, and 10 healthy individuals, as well as 2 patients with isolated inner dynein arm defects, had normal

DNAH5 staining (Table 1). We conclude that DNAH5 staining of respiratory epithelial cells can detect ODA defects.

Correlation of Total and Distal DNAH5 Deficiency in the Ciliary Axoneme with Residual Ciliary Motility

The functional relevance of distal and complete DNAH5 deficiency within the respiratory ciliary axoneme of patients with PCD becomes evident by correlation with the beat frequency and pattern (Table 1; *see* the online supplement for supplementary video). Among the 13 patients with PCD with complete axonemal absence of DNAH5 and available high-speed video microscopic
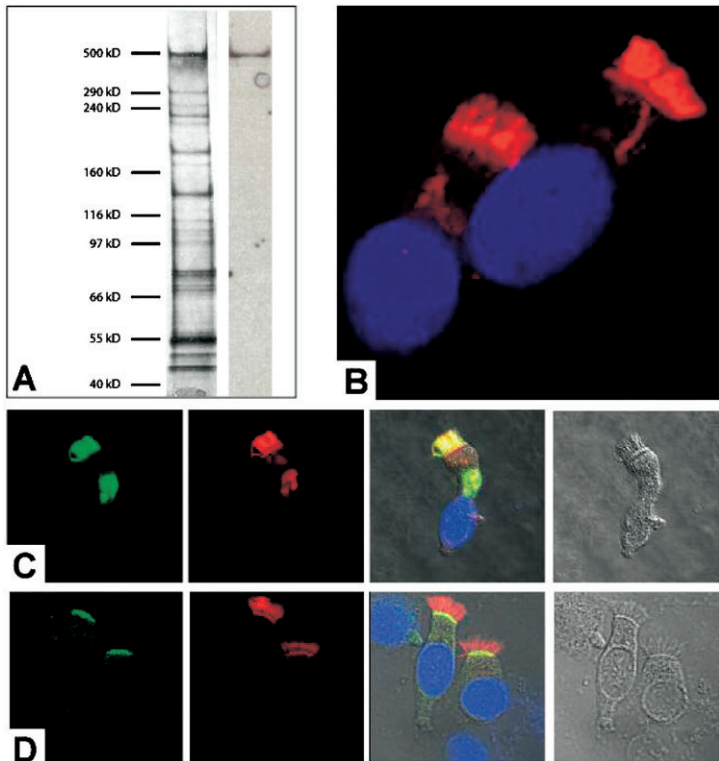
Figure 1. Specific antibodies localize the human axonemal outer dynein arm heavy chain DNAH5 to the ciliary axoneme, the microtubule-organizing centers, and cytosolic compartments of respiratory epithelial cells. (*A*) Silver staining (*left*) and Western blot analysis (*right*) of axonemal protein extracts from pig trachea. High molecular mass bands (about 500 kD) represent the axonemal dynein heavy chains. DNAH5 antibodies specifically detect a single band with the predicted size. (*B–D*) Immunofluorescence staining of human respiratory epithelial cells with DNAH5-specific antibodies (*red*). Costaining with antibodies against axoneme-specific acetylated α-tubulin (*C*) and γ-tubulin, which stains the microtubule-organizing centers in the vicinity of the basal body (*D*), was used as control (*green*). Nuclei were stained with Hoechst 33342 (*blue*). Overlays and bright-field images are shown on the *right* in (*C*) and (*D*).

data, cilia immotility was observed in 12 patients. Only one patient had severely reduced beat frequency. Cilia with distal DNAH5 deficiency showed a residual motion of 1–5 Hz (in five of six patients), and immotility in only one patient. All cilia with residual activity showed abnormal coordination and limited range of bending.

Sperm Analyses in a Patient with *DNAH5* Mutations Reveal Sperm Immotility without Alterations of DNAH5 Content within the Flagellar Axoneme

Repeated spermiograms of two brothers with PCD carrying *DNAH5* mutations revealed in F373-II3 low sperm counts (oligozoospermia) and immotile sperm tails (*see* the online supplement for supplementary video), and in patient F373-II4 an absence of sperm cells (azoospermia) (Table 1). To test whether similar defects account for ciliary and flagellar dyskinesia, we first examined the DNAH5 and DNAH9 distribution in human wild-type sperm cells. The staining pattern of the two ODA heavy chains differed in wild-type sperm cells and respiratory cilia. DNAH5 stained the proximal half of the flagellar axoneme whereas DNAH9 staining was observed along the entire flagellum (Figure 4). We then analyzed DNAH5-mutant sperm cells from patient F373-II3. In

contrast to respiratory epithelial cells from this patient (Figure 3A), we did not detect any differences of the staining pattern compared with wild-type sperm flagella (Figure 4).

DISCUSSION

ODA multiprotein complexes are large molecular motors that generate the energy for bending of motile cilia and flagella. In *Chlamydomonas* the ODA is invariably composed of three heavy chains (α-, β-, and γ-heavy chain) that form the globular motor domain and the stem, two intermediate chains (IC69 and IC78) at the base of the complex, and eight light chains (4–6). In addition, an ODA-docking complex comprising three proteins attaches the ODA onto the microtubules (20). To investigate the molecular mechanisms involved in human ODA generation and function we used specific antibodies against different ODA components to stain respiratory epithelial and sperm cells. Confocal immunofluorescence imaging reveals characteristic patterns of ciliary and subcellular localization of the various analyzed ODA components. In wild-type respiratory cells the ODA heavy chain DNAH5 is present throughout the entire length of the ciliary axoneme, whereas the ODA heavy chain DNAH9 localizes
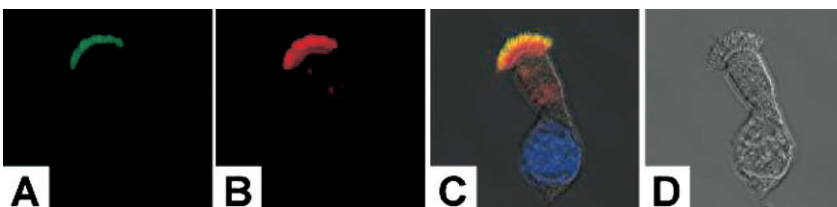

Figure 2. DNAH9 localizes exclusively to distal parts of respiratory ciliary axonemes: costaining of human respiratory epithelial cells with antibodies against axonemal ODA heavy chains DNAH9 (*green*) and DNAH5 (*red*). DNAH5 localizes along the entire length of the axonemes, within the microtubule-organizing centers, and specific cytosolic compartments. Nuclei were stained with Hoechst 33342 (*blue*). (*A*) DNAH9 staining; (*B*) DNAH5 staining; (*C*) overlay; and (*D*) bright-field image.
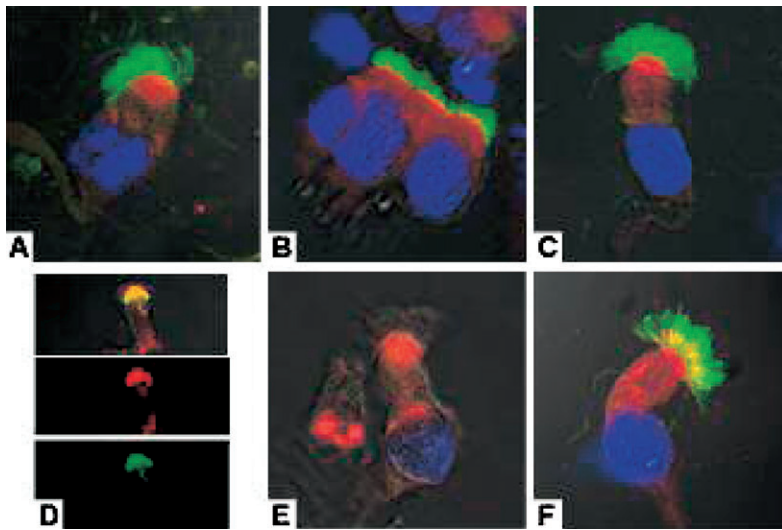
Figure 3. Mislocalization of ODA components in respiratory epithelial cells from patients with PCD with *DNAH5* and *DNAI1* mutations: overlay images of respiratory epithelial cells from patients with PCD carrying the *DNAH5* mutations (*A*) 1855NfsX5, (*B*) 2814fsX1, and (*C*) IVS74-1G→C, co-stained with antibodies against DNAH5 (*red*) and acetylated α-tubulin (*green*). Nuclei were stained with Hoechst 33342 (*blue*). Mutant DNAH5 (*A*–*C*) is expressed and localizes correctly to the ODA preassembly site at the microtubule-organizing centers but is unable to enter the ciliary compartment. Note that the mutant protein accumulates within the cytosolic DNAH5 compartments including the proximal perinuclear region and the expanded microtubule-organizing centers. (*D*) Colocalization of DNAH5 (*red*) and γ-tubulin (*green*) in respiratory epithelial cells from a patient with PCD with mutant DNAH5 (1855NfsX5), demonstrating expansion of the microtubule-organizing centers. The overlay (*yellow*) is shown at the *top*. (*E*) Overlay image of respiratory cells from a patient with the *DNAH5* mutation 1855NfsX5. DNAH9 (*green*) is absent from the ciliary axonemes. Only weak and diffuse DNAH9 staining is detected within the cytoplasm. DNAH5 (*red*) is also absent within the ciliary axoneme but accumulates in the microtubule-organizing centers. (*F*) Overlay image of a respiratory cell from a patient with a mutation of the ODA intermediate chain gene *DNAI1* (219+3insT/W568X). The ciliary axoneme is stained with acetylated α-tubulin (*green*). DNAH5 (*red*) is undetectable in the distal part of the axonemes but accumulates in the cytoplasmic compartments. *Yellow* within the proximal ciliary axoneme indicates that both proteins are present in these regions.
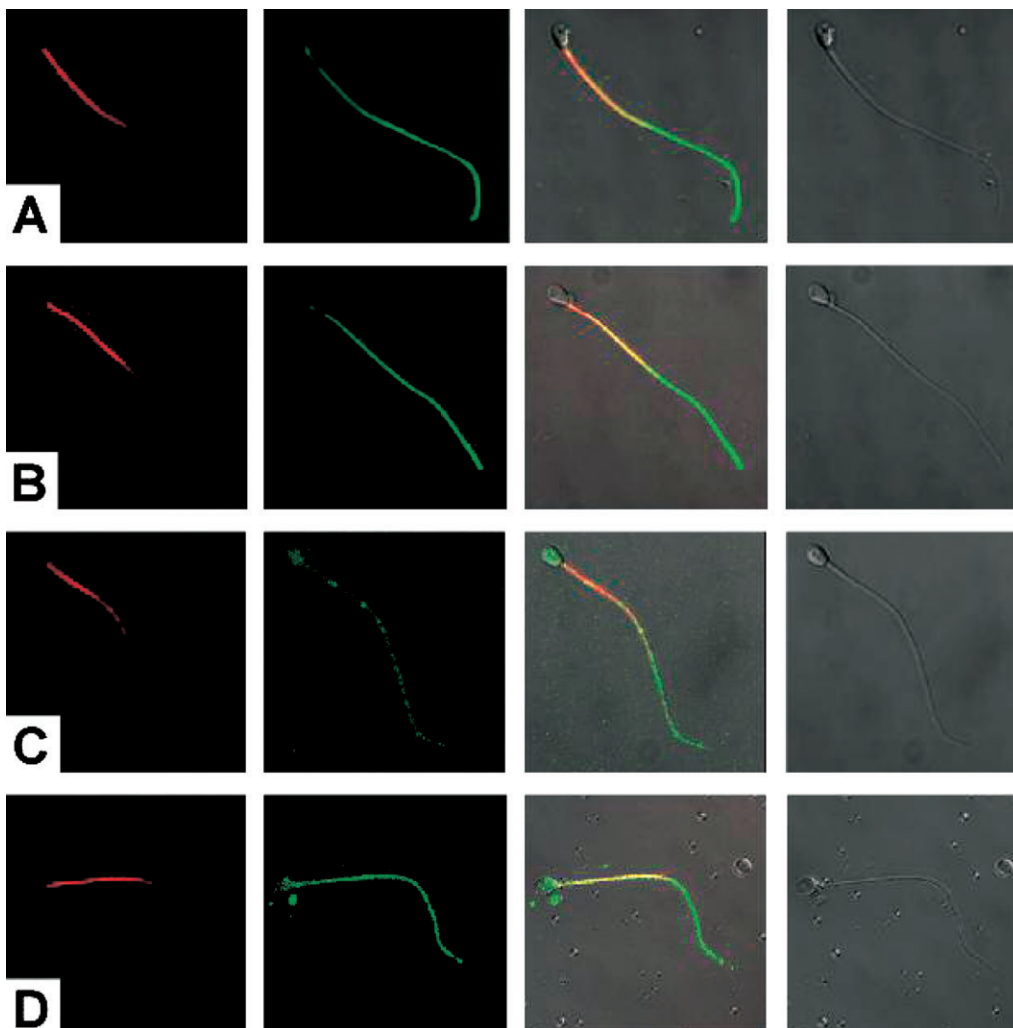

Figure 4. The spatial distribution of ODA heavy chains DNAH5 and DNAH9 in sperm tails remains unchanged in a patient with PCD carrying a homozygous *DNAH5* mutation. (*A* and *B*) Spermatozoa were costained with antibodies against DNAH5 (*red*) and acetylated α-tubulin (*green*). (*C* and *D*) Costaining of DNAH5 (*red*) and DNAH9 (*green*). (*A* and *C*) Sperm cells from a healthy donor. (*B* and *D*) Sperm cells from PCD patient F373-II3. Overlay and bright-field images are shown on the *right*. DNAH5 localizes exclusively to the proximal part of the sperm tail, whereas DNAH9 localizes to the entire sperm axoneme in both wild-type and DNAH5 mutant sperm. In contrast to respiratory cilia, the distribution of ODA heavy chains in sperm axonemes is not influenced by the *DNAH5* mutation in F373-II3.

exclusively to the distal ciliary compartment (Figure 2). In contrast, in sperm cells DNAH5 localizes only to the proximal part of the flagellum, whereas DNAH9 antibodies stain the entire length of the sperm tail (Figure 4). These findings demonstrate for the first time that ODA complexes vary in their composition along the respiratory ciliary axoneme and the axoneme of the sperm tail, and that this composition also differs between these two cell types. Our data indicate that in respiratory cilia at least two ODA types are present: Type 1 (DNAH9 negative and DNAH5 positive; proximal ciliary axoneme) and Type 2 (DNAH9 and DNAH5 positive; distal ciliary axoneme). We assume that the spatial diversity of ODA heavy chains along the axonemes most likely contributes to the typical beating characteristics of cilia and sperm flagella and likewise to the various beat modes of other motile cilia types (e.g., ependymal and nodal cilia). Because of the limited availability of antibodies, we focused our analysis on two ODA heavy chains. However, comparative genome analyses identified at least four human ODA heavy chains (21, 22), indicating an even higher variability of ODA composition in human cilia.

We investigated the molecular mechanisms by which mutations within genes (*DNAH5* and *DNAI1*) encoding ODA components cause PCD (9, 11). In *DNAH5* mutant respiratory epithelial cells from three patients with PCD we found that the truncated DNAH5 proteins are absent within the ciliary compartment. These axonemes also lack DNAH9 (Figure 3), indicating that both ODA complexes are affected. We regularly observed only immotile cilia in respiratory epithelial cells of these patients (Table 1; *see* the online supplement for supplementary video). Because the F373 frameshift mutation (1855NfsX5) predicts the loss of two-thirds of DNAH5 we conclude that the recognition signal responsible for targeting of DNAH5 to the microtubule-organizing centers region is located in the N-terminal part of the protein. Similar to our observations in *DNAH5* mutant cells, mutations of the intermediate chain gene *DNAI1* also caused an accumulation of DNAH5 at the microtubule-organizing centers in respiratory cells of patient UNC119 (Figure 3F). However, in this case DNAH5 staining was negative only in the distal part of the axonemes; it was positive in the proximal part. DNAH9, which sublocalizes to the distal part in wild-type cells, was absent throughout the ciliary compartment. Thus the studied *DNAI1* mutations affect Type 2 ODA complexes (DNAH5 and DNAH9 positive in the distal part of the axoneme), whereas Type 1 ODA complexes (DNAH5 positive and DNAH9 negative in the proximal ciliary axoneme) appear unaffected. This correlates with our functional data showing that defects affecting mainly one ODA type show significantly more cells with cilia motility, compared with defects that affect both ODA types (Table 1). In conclusion, these results demonstrate that at least two distinct ODA types are present within human respiratory cilia, and that they can be affected by PCD gene mutations either alone or together. Because we studied respiratory cells of only a limited number of patients with known PCD gene mutations, further studies are needed to clarify whether *DNAI1* and *DNAH5* mutations in general result in a distinct pattern of DNAH5 mislocalization.

Fortunately, we were also able to study sperm function and morphology in a patient with known *DNAH5* mutations. We could demonstrate for patient F373-II3 that a homozygous truncational *DNAH5* mutation results in sperm immotility (*see* the online supplement for a supplementary video), and expected that *DNAH5* mutant sperm flagella from this proband completely lack DNAH5 and DNAH9 as observed in respiratory cilia from the same individual (Figure 3A). However, we found that DNAH5 and DNAH9 content were indistinguishable from that of wild-type sperm cells (Figure 4). We assume that sperm

immotility probably results from a functional defect of the truncated DNAH5 protein (1855NfsX5), which lacks the entire C-terminal motor domain, similar to mutations of the *DNAH5* ortholog in *Drosophila,* which cause infertility of male flies (23–25). We assume that, similar to previously described mechanisms in *Chlamydomonas* (26), human ODA components probably preassemble within the cytoplasm and are delivered as ODA precursors to the ciliary compartment of respiratory cilia, and that this process is altered by mutant ODA proteins. This is supported by the fact that mutant DNAH5 is still correctly targeted to the microtubule-organizing centers, where it strongly accumulates instead of entering the ciliary compartment (Figure 3). Lack of assembly of ODA precursors at their docking sites within the ciliary compartment is less likely to explain our observations, because DNAH5 and DNAH9 are correctly localized within the flagellar axoneme of sperm tails. How can we explain that sperm and respiratory cells carrying identical mutations (F373-II3) show distinct phenotypes regarding the content of ODA heavy chains along the axoneme? In *Chlamydomonas*, trafficking of flagella-specific proteins between the two separated cytoplasmic and flagellar compartments is accomplished by the intraflagellar transport machinery (27). The process of assembly and maintenance of cilia and flagella by transport particles passing the compartment borders has been described as "compartmentalized ciliogenesis" (28). Possibly human sperm tail generation resembles "cytosolic ciliogenesis" as observed in *Drosophila*, which is independent of intraflagellar transport.

Diagnosis of PCD is currently based on (*1*) a typical clinical presentation, including recurrent respiratory infections with or without situs inversus, and (*2*) ciliary dyskinesia or sperm immotility assessed by light microscopy and/or demonstration of specific axonemal ultrastructural defects by electron microscopy (2). However, diagnosis is often difficult and delayed (29). Several factors contribute to this clinical problem. First, ciliary activity assessed by light microscopy might be altered as a result of secondary changes caused by concomitant infections. Second, electron microscopy is performed in many laboratories exclusively on samples obtained by more elaborate procedures such as transnasal clamp biopsies (conchae) or bronchoscopy (bronchial airway material). In addition, some ultrastructural changes might also be influenced by secondary ciliary changes (30). Therefore, research currently focuses on novel techniques to ascertain PCD diagnosis. For that purpose we evaluated the potential role of DNAH5 staining for the diagnosis of PCD with ODA defects, which are the most common ultrastructural abnormalities encountered in PCD (30). Our data demonstrate that DNAH5 staining of respiratory epithelial cells obtained by transnasal brushings can detect ODA defects (Table 1). This novel method has two advantages. First, immunofluorescence staining is performed in respiratory epithelial cells obtained by noninvasive transnasal brushings. In addition, this material can be used at the same time for functional analysis of ciliary beat frequency and pattern, which avoids additional samplings. Second, the method is able to detect changes along the entire ciliary axoneme. This aspect is of particular significance, because with transmission electron microscopy localization of the examined cross-sections along the ciliary axoneme is not possible. The demonstration that in some patients the ODA component DNAH5 is not localized to the ciliary axoneme at all (defect of both ODA types), and in others that DNAH5 is still present in the proximal parts of the ciliary compartment (defect of only ODA Type 2), might explain the variability of ultrastructural defects observed in PCD (31).

In conclusion, we demonstrate for the first time that mutations responsible for ciliary defects cause altered localization of axonemal proteins within the ciliary compartment. We anticipate that other ultrastructural defects of, for example, inner dynein

arms and radial spokes also observed in PCD are caused by similar molecular mechanisms.

References

1. Ibanez-Tallon I, Heintz N, Omran H. To beat or not to beat: roles of cilia in development and disease. *Hum Mol Genet* 2003;12:27–35.

2. Afzelius BA, Mossberg B, Bergström SE. Immotile cilia syndrome (primary ciliary dyskinesis), including Kartagener syndrome. In: Scriver CS, Beaudet AL, Valle D, Sly WS, Childs B, Kinzler KW, Vogelstein B, editors. The metabolic and molecular bases of inherited disease, 8th ed. Vol. 3. New York: McGraw-Hill; 2001. pp. 4817–4827.

3. El Zein L, Omran H, Bouvagnet P. Lateralization defects and ciliary dyskinesia: lessons from algae. *Trends Genet* 2003;19:162–167.

4. Holzbaur EL, Vallee RB. Dyneins: molecular structure and cellular function. *Annu Rev Cell Biol* 1994;10:339–372.

5. Witman GB, Wilkerson CG, King SM. The biochemistry, genetics and molecular biology of flagellar dynein. In Hyams JS, Lloyd CW, editors. Microtubules. New York: Wiley-Liss; 1994. pp. 229–249.

6. DiBella LM, King SM. Dynein motors of the *Chlamydomonas* flagellum. *Int Rev Cytol* 2001;210:227–268.

7. Omran H, Haffner K, Volkel A, Kuehr J, Ketelsen U-P, Ross UH, Konietzko N, Wienker T, Brandis M, Hildebrandt F. Homozygosity mapping of a gene locus for primary ciliary dyskinesia on chromosome 5p and identification of the heavy dynein chain DNAH5 as a candidate gene. *Am J Respir Cell Mol Biol* 2000;23:696–702.

8. Wilkerson CG, King SM, Witman GB. Molecular analysis of the γ heavy chain of *Chlamydomonas* flagellar outer-arm dynein. *J Cell Sci* 1994;107:497–506.

9. Olbrich H, Haffner K, Kispert A, Volkel A, Volz A, Sasmaz G, Reinhardt R, Hennig S, Lehrach H, Konietzko N, *et al.* Mutations in DNAH5 cause primary ciliary dyskinesia and randomization of left–right asymmetry. *Nat Genet* 2002;30:143–144.

10. Wilkerson CG, King SM, Koutoulis A, Pazour GJ, Witman GB. The 78,000 M_r intermediate chain of *Chlamydomonas* outer arm dynein is a WD-repeat protein required for arm assembly. *J Cell Biol* 1995;129:169–178.

11. Pennarun G, Escudier E, Chapelin C, Bridoux AM, Cacheux V, Roger G, Clement A, Goossens M, Amselem S, Duriez B. Loss-of-function mutations in a human gene related to *Chlamydomonas reinhardtii* dynein IC78 result in primary ciliary dyskinesia. *Am J Hum Genet* 1999;65:1508–1519.

12. Reed W, Carson JL, Moats-Staats BM, Lucier T, Hu P, Brighton L, Gambling TM, Huang CH, Leigh MW, Collier AM. Characterization of an axonemal dynein heavy chain expressed early in airway epithelial ciliogenesis. *Am J Respir Cell Mol Biol* 2000;23:734–741.

13. Hastie AT. Isolation of respiratory cilia. *Methods Cell Biol* 1995;47:93–98.

14. Sisson JH, Stoner JA, Ammons BA, Wyatt TA. All-digital image capture and whole-field analysis of ciliary beat frequency. *J Microsc* 2003;211:103–111.

15. O'Toole ET, Giddings TH, McIntosh JR, Dutcher SK. Three-dimensional organization of basal bodies from wild-type and δ-tubulin deletion strains of *Chlamydomonas reinhardtii*. *Mol Biol Cell* 2003;14:2999–3012.

16. Dutcher SK. Elucidation of basal body and centriole functions in *Chlamydomonas reinhardtii*. *Traffic* 2003;4:443–451.

17. Muresan V, Joshi HC, Besharse JC. γ-Tubulin in differentiated cell types: localization in the vicinity of basal bodies in retinal photoreceptors and ciliated epithelia. *J Cell Sci* 1993;104:1229–1237.

18. Guichard C, Harricane MC, Lafitte JJ, Godard P, Zaegel M, Tack V, Lalau G, Bouvagnet P. Axonemal dynein intermediate-chain gene (*DNAI1*) mutations result in situs inversus and primary ciliary dyskinesia (Kartagener syndrome). *Am J Hum Genet* 2001;68:1030–1035.

19. Zariwala M, Noone PG, Sannuti A, Minnix S, Zhou Z, Leigh MW, Hazucha M, Carson JL, Knowles MR. Germline mutations in an intermediate chain dynein cause primary ciliary dyskinesia. *Am J Respir Cell Mol Biol* 2001;25:577–583.

20. Takada S, Wilkerson CG, Wakabayashi K, Kamiya R, Witman GB. The outer dynein arm-docking complex: composition and characterization of a subunit (oda1) necessary for outer arm assembly. *Mol Biol Cell* 2002;13:1015–1029.

21. Chapelin C, Duriez B, Magnino F, Goossens M, Escudier E, Amselem S. Isolation of several human axonemal dynein heavy chain genes: genomic structure of the catalytic site, phylogenetic analysis and chromosomal assignment. *FEBS Lett* 1997;412:325–330.

22. Maiti AK, Mattei MG, Jorissen M, Volz A, Zeigler A, Bouvagnet P. Identification, tissue specific expression, and chromosomal localisation of several human dynein heavy chain genes. *Eur J Hum Genet* 2000;8:923–932.

23. Gepner J, Hays TS. A fertility region on the Y chromosome of *Drosophila melanogaster* encodes a dynein microtubule motor. *Proc Natl Acad Sci USA* 1993;90:11132–11136.

24. Rasmusson K, Serr M, Gepner J, Gibbons I, Hays TS. A family of dynein genes in *Drosophila melanogaster*. *Mol Biol Cell* 1994;5:45–55.

25. Carvalho AB, Lazzaro BP, Clark AG. Y chromosomal fertility factors kl-2 and kl-3 of *Drosophila melanogaster* encode dynein heavy chain polypeptides. *Proc Natl Acad Sci USA* 2000;97:13239–13244.

26. Fowkes ME, Mitchell DR. The role of preassembled cytoplasmic complexes in assembly of flagellar dynein subunits. *Mol Biol Cell* 1998;9:2337–2347.

27. Rosenbaum JL, Witman GB. Intraflagellar transport. *Nat Rev Mol Cell Biol* 2002;3:813–825.

28. Avidor-Reiss T, Maer AM, Koundakjian E, Polyanovsky A, Keil T, Subramaniam S, Zuker CS. Decoding cilia function: defining specialized genes required for compartmentalized cilia biogenesis. *Cell* 2004;117:527–539.

29. Bush A. Primary ciliary dyskinesia. *Acta Otorhinolaryngol Belg* 2000;54:317–324.

30. Jorissen M, Willems T, Van der Schueren B, Verbeken E, De Boeck K. Ultrastructural expression of primary ciliary dyskinesia after ciliogenesis in culture. *Acta Otorhinolaryngol Belg* 2000;54:343–356.

31. Noone PG, Leigh MW, Sannuti A, Minnix SL, Carson JL, Hazucha M, Zariwala MA, Knowles MR. Primary ciliary dyskinesia: diagnostic and phenotypic features. *Am J Respir Crit Care Med* 2004;15:459–467.